MODELADO DE GRIETAS DE INTERFASE EN UN COMPOSITE CON UN GRUPO DE FIBRAS SOMETIDO A CARGAS TRANSVERSALES BIAXIALES

MODELLING OF INTERFACE CRACKS IN A COMPOSITE WITH A FIBRE BUNDLE UNDER BIAXIAL TRANSVERSE LOADS

L. Távara, V. Mantič, E. Graciani, F. París

Grupo de Elasticidad y Resistencia de Materiales,
Escuela Técnica Superior de Ingenieros, Universidad de Sevilla,
Camino de los Descubrimientos s/n, 41092 Sevilla, España.
E-mail: ltavara@us.es, mantic@us.es, egraciani@us.es, fparis@us.es

RESUMEN

En el presente trabajo se presenta un estudio numérico donde se caracteriza el inicio y crecimiento de los despegues producidos en las interfases entre fibra y matriz en un material compuesto sometido a cargas transversales biaxiales. Se considera un problema simplificado que representa una lámina unidireccional real, con diez fibras embebidas en una matriz cuyas dimensiones externas son mucho más grandes que el radio de las fibras. Con este análisis se amplia, por tanto, los resultados obtenidos por los autores en trabajos previos en que se empleaba un problema con una sola fibra. El objetivo es, por un lado, predecir las cargas de fallo (cargas críticas) para un pequeño grupo de fibras y, por otro, verificar el crecimiento inestable de los despegues correspondientes a estas cargas críticas. La curva de fallo obtenida para este problema simplificado permite dilucidar algunos aspectos de la curva de fallo de un material compuesto real sometido a cargas transversales.

ABSTRACT

A numerical study of debond onset and growth at fibre–matrix interfaces in a fibre bundle under biaxial transversal loads is presented. A simplified but representative problem of an actual unidirectional lamina is considered, with ten fibres embedded in a matrix with external dimensions much larger than the fibre radii. The results presented extended the results obtained by the authors in previous works, where a single fibre problem was studied. The aim is, first, to predict the failure loads (critical loads) for a small bundle of fibres and, second, to verify the unstable character of debond growth under transverse loads. The failure curve obtained in this simplified problem helps in elucidating some aspects of the failure mechanisms of an actual composite material subjected to these loads.

PALABRAS CLAVE: Composites, Mixed mode fracture, Interface crack

1. INTRODUCTION

Experimental, numerical and semi-analytical studies of the inter-fibre failure (also called matrix failure) of a unidirectional composite lamina under biaxial transverse loads developed by the present authors and coworkers are presented in several works [1, 2, 3, 4, 5]. These works show the influence of a secondary transversal load (tension or compression) applied perpendicularly to the primary transverse tension (thus creating a biaxial state) on the generation of the damage dominated by the primary transverse tension. Numerical models of a single fibre embedded in a large matrix, based on Boundary Element Method (BEM) [6] and interfacial fracture mechanics, are presented in [7, 8].

The present authors, in some recent works [9, 10, 11], have made a step forward in the quantitative prediction of the influence of the secondary transversal load in the above mentioned problem, obtaining a failure curve in which both tensile and compressive loads are considered for a single fibre configuration. BEM and Linear Elastic-Brittle Interface Model (LEBIM) are used to study and characterize the behavior of the fibre-matrix interface in these works.

The aim of the present work is to make a new step forward regarding the inter-fibre failure of a unidirectional composite lamina, by modelling (using BEM and LEBIM) a more representative problem of an actual unidirectional lamina, with a bundle of ten fibres embedded in a matrix whose external dimensions are much larger than the radius of fibres. An extensive review of the literature about the problem of an elastic circular inclusion embedded in an elastic matrix with or without a partial debond can be found in [10]. Details of the LEBIM implementation in a BEM code are also presented therein. Additional details about the weak formulation used to impose interface conditions are presented in [12, 13]. Some fundamental results regarding the computation of the Energy Release Rate (ERR) in the LEBIM can be found in [14, 15].

The present paper is organized as follows. First the LE-

BIM used and the interface failure criterion are briefly described. Then, a plane strain problem of a group of circular inclusions, representing a bundle of long fibres under a remote biaxial transversal loading, is introduced. BEM is applied to the numerical solution of fibre-matrix interface crack onset and growth in this problem. The numerical results include a study of the crack path formed by the debonds in the fibre-matrix system. Finally, failure curves of a bundle of fibres under biaxial transversal loads are obtained.

2. INTERFACE FAILURE CRITERION

As shown in [9, 10, 11], the LEBIM can be used in microscale models to simulate the damage initiation and propagation at the fibre-matrix interface. In this section, the LEBI constitutive law and the interface failure criterion developed in [9, 10, 11, 16] are briefly reviewed. The continuous spring distribution that models the elastic layer (interphase) along the fibre-matrix interface is governed by the following simple linear elastic- (perfectly) brittle law written at an interface point x:

$$\begin{array}{ll} \text{Linear Elastic interface} & \left\{ \begin{array}{l} \sigma(x) = k_n \delta_n(x) \\ \tau(x) = k_t \delta_t(x) \end{array} \right. \quad t(x) < t_c(\psi_\sigma(x)) \\ \text{Broken interface} & \left\{ \begin{array}{l} \sigma(x) = \left\langle \begin{array}{ll} 0 & \delta_n(x) > 0 \\ k_n \delta_n(x) & \delta_n(x) \le 0 \end{array} \right. \\ \tau(x) = 0 \end{array} \right. \end{array} \tag{1}$$

where $\sigma(x)$ and $\tau(x)$ are, respectively, the normal and tangential components of the tractions along the interface in the elastic layer, $\delta_n(x)$ and $\delta_t(x)$ are, respectively, the normal and tangential relative displacements between opposite interface points. k_n and k_t denote the normal and tangential stiffnesses of the spring distribution. The traction modulus t is defined as $t(x) = \sqrt{\sigma^2(x) + \tau^2(x)}$. The critical traction modulus t_c adopted is deduced in the following.

The ERR of the linear elastic interface at a point x is defined as: $G(x) = G_I(x) + G_{II}(x)$ if $\sigma > 0$ and $G(x) = G_{II}(x)$ if $\sigma \le 0$, with

$$G_I(x) = \frac{\sigma(x)\delta_n(x)}{2}, \qquad G_{II}(x) = \frac{\tau(x)\delta_t(x)}{2}. \tag{2}$$

The fracture mode mixity angle ψ_σ at an interface point x is defined by $\tan\psi_\sigma(x) = \tau(x)/\sigma(x)$. It is assumed that the crack tip at x advances (or an interface point x breaks) when the corresponding ERR $G(x)$ reaches the critical ERR value $G_c(\psi_\sigma(x))$, that is $G(x) = G_c(\psi_\sigma(x))$. The functional dependence of G_c on the fracture mode mixity angle ψ_σ can be defined similarly as in [17] with a slight modification [11] as follows,

$$G_c = G_{Ic}[1 + \tan^2((1-\lambda)\tilde{\psi})], \tag{3}$$

where

$$G_{Ic} = \frac{\bar{\sigma}_c \bar{\delta}_{nc}}{2} = \frac{\bar{\sigma}_c^2}{2k_n} = \frac{k_n \bar{\delta}_{nc}^2}{2} \tag{4}$$

corresponds to the fracture energy in pure opening mode I. λ is a fracture-mode-sensitivity parameter (usually obtained from the best fit of experimental results), $\bar{\sigma}_c$ and $\bar{\delta}_c$ are the critical normal component of traction and normal relative displacement in mode I, i.e. $\bar{\sigma}_c = \sigma_c(\psi_\sigma = 0)$. $\tilde{\psi} = \tilde{\psi}(\psi_\sigma)$ is a smooth continuous function defined as

$$\left\{ \begin{array}{ll} \arctan\{\sqrt{\frac{k_n}{k_t}}\tan\psi_\sigma\} & |\psi_\sigma| < \pi/2 \\ \pm\pi/2 & \psi_\sigma = \pm\pi/2 \\ \pi\,\mathrm{sgn}\,\psi_\sigma + \arctan\{\sqrt{\frac{k_n}{k_t}}\tan\psi_\sigma\} & \pi/2 < |\psi_\sigma| \le \pi \end{array} \right. \tag{5}$$

sgn being the signum function.

Using this energy based criterion, the critical traction modulus t_c is defined as $t_c(\psi_\sigma(x)) = \sqrt{\sigma_c^2(\psi_\sigma) + \tau_c^2(\psi_\sigma)}$, with the general expressions of the critical normal and tangential components of the traction defined, as functions of ψ_σ,

$$\sigma_c(\psi_\sigma) = \bar{\sigma}_c \sqrt{1 + \tan^2[(1-\lambda)\tilde{\psi}]}\,\cos\tilde{\psi}, \tag{6}$$

$$\tau_c(\psi_\sigma) = \sqrt{\frac{k_t}{k_n}}\bar{\sigma}_c \sqrt{1 + \tan^2[(1-\lambda)\tilde{\psi}]}\,\sin\tilde{\psi}. \tag{7}$$

Finally, it can be seen that the LEBIM needs the input of four independent variables: $\bar{\sigma}_c$, G_{Ic}, k_n/k_t ratio and λ. Typical range $0.2 \le \lambda \le 0.35$ characterizes interfaces with moderately strong fracture mode dependence [17]. Further details of the above criterion deduction are presented in [9, 10, 16].

3. DESCRIPTION OF THE PROBLEM

In the present study a bundle of ten infinitely long cylindrical inclusions, with a circular section of radius a, are considered embedded in an infinite matrix. The position of the fibres correspond to a portion of an actual glass fibre composite micrograph [1], see Figure 1.

Both the inclusions and the matrix are considered as linear elastic isotropic materials. Let (x, y, z) be the cartesian coordinates, the z-axis being the longitudinal axis of the inclusion. The uniform remote loads σ_x^∞ and σ_y^∞ are parallel to the x-axis (horizontal) and y-axis (vertical), respectively.

Remote loads $\sigma_y^\infty > 0$ and σ_x^∞ are applied along the sides of a large square matrix that surrounds the bundle of fibres (located approximately at the centre of the square) for different values of the biaxiality ratio μ,

$$\mu = \frac{\sigma_x^\infty + \sigma_y^\infty}{2[\text{máx}(|\sigma_x^\infty|, |\sigma_y^\infty|)]} \tag{8}$$

where $\mu = -0.5$ describes a pure compressive state in one direction and $\mu = 0.5$ describes a pure traction state in one direction. $-0.5 \le \mu \le 1$ values are considered in the present work. In order to see the influence of the random

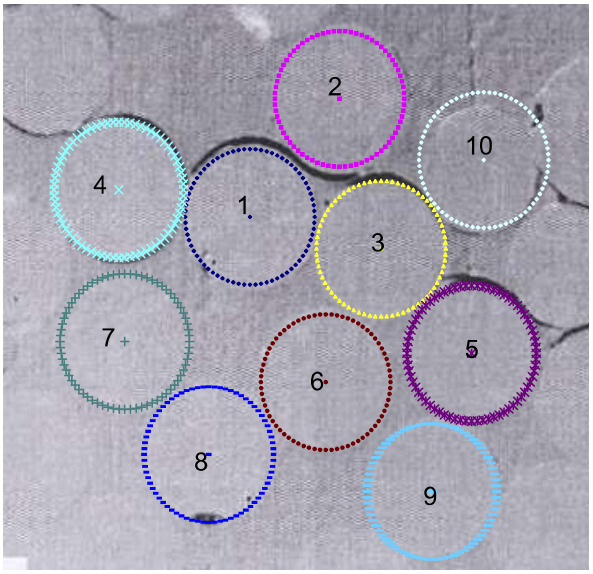

Figure 1: Selected fibres obtained from a glass fibre composite micrograph.

positions of fibres, the bundle of fibres has been rotated 15°, 30°, 45°, 60° and 75° with respect to the x-axis. As mentioned above, a plane strain state is assumed in the present bimaterial system.

4. MODEL OF THE PROBLEM

A typical bimaterial system among fibre reinforced composite materials is chosen for this study: epoxy matrix (m) and glass fibre (f). The elastic properties of matrix and fibre are $E_m = 2.79$ GPa, $\nu_m = 0.33$, $E_f = 70.8$ GPa and $\nu_f = 0.22$. The corresponding Dundurs' bimaterial parameters are $\alpha = 0.919$ and $\beta = 0.229$, and the harmonic mean of the effective elasticity moduli in plane strain $E^* = 6.01$GPa, see [7, 8, 18].

The fracture and strength properties of the interface assumed in the present work are: the fibre-matrix interface fracture toughness in mode I, $G_{Ic} = 2\text{Jm}^{-2}$, and the critical tension $\bar{\sigma}_c = 90$MPa. These values are chosen because they are in the range of values found in the literature [18, 19, 20] and simulate a brittle interface behavior as stated in [10], making the hypothesis of the LEBIM to appropriately represent a possible real composite material behavior. A fixed relation between k_n and k_t ($k_t = k_n/4$) is chosen. The fracture-mode-sensitivity parameter is $\lambda = 0.25$. The influence of these variables in the single fibre problem have been studied in detail in [10, 11].

The 2D BEM model represents ten circular inclusions with a radius a =7.5 μm inside a relatively large square matrix with a 1 mm side. 3632 continuous linear boundary elements are used: 32 elements for the external boundary of the matrix and two uniform meshes (for each fibre) of 180 elements to model the fibre-matrix interface (therefore, the polar angle of each element is 2°).

After the initial definition of the undamaged interfaces, a linear analysis is carried out to calculate which interface node (spring) reaches first its critical traction modulus value. This linear analysis will be the first step and the calculated critical load corresponds to the load that causes the debond onset. Then, the solution algorithm makes a sequence of similar linear analyses where the interface points (springs) that have reached the critical value in the previous step changes its interface condition (broken spring). Each linear analysis becomes a new step and its critical load corresponds to the load that causes a new debond growth.

5. NUMERICAL RESULTS

In the following sections we will discuss the numerical results obtained in the different analyses carried out using the BEM model described above.

5.1. *Debond onset and growth*

Figure 2 shows the values of the far-field load needed for the first debond onset (first step) and the load needed in each subsequent step to produce either a debond growth or an onset of a new debond for the case with $\mu = 0.5$ (uniaxial loading in the y-direction) and no rotation of the bundle of fibres. A limit line corresponding to the (first) critical load σ_{cy}^{∞} (the critical load in the y direction) is showed with a dotted line in the figure. Notice that, the step number could easily be related with the summation of the debond angles along all the different fibre-matrix interfaces. This is due to the fact that the solution algorithm applied "breaks" only one interface spring in each step. Therefore, as all the elements at fibre-matrix interfaces are of the same size, each step essentially represents an increase of the total debond length by an arc length corresponding to the polar angle of 2°.

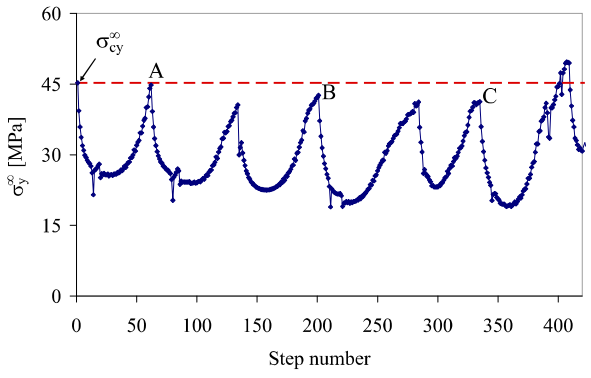

Figure 2: Far-field load needed in each step to produce either a debond onset or debond growth for a load biaxiality ratio $\mu = 0.5$.

Regarding the way the debond growth occurs it is useful to recall that one of the main conclusions obtained in the previous studies (considering a single fibre model) was that the debond growth initially occurs in an unstable manner (a snap-back or snap-through is produced). Thus, once a critical load its reached, lower loads are needed to cause the subsequent interface crack growth [10, 11]. This fact is observed again in the present multi-fibre model, see Figure 2, where a sequence of local unstable growths (a serie of picks and valleys) occurs, each of them corresponding to a debond onset and unstable growth at a different fibre. The sequence of the debonds in this case is given by fibre numbers: 5, 6, 4, 1 and 3 (numbering according to Figure 1).

In Figure 3, the deformed shape (at the scale of the fibres) of the solved problem multiplied by a factor of two is shown for 3 different steps. These steps are marked with letters A, B and C in Figure 2 and correspond to step numbers 62, 201 and 358 respectively. Although, the present BEM code does not have the capability to let interface cracks to kink into the matrix and coalesce, a well defined crack path can be clearly seen in Figure 3(c) that may produce (after a coalescence of the debonds) a macro-crack.

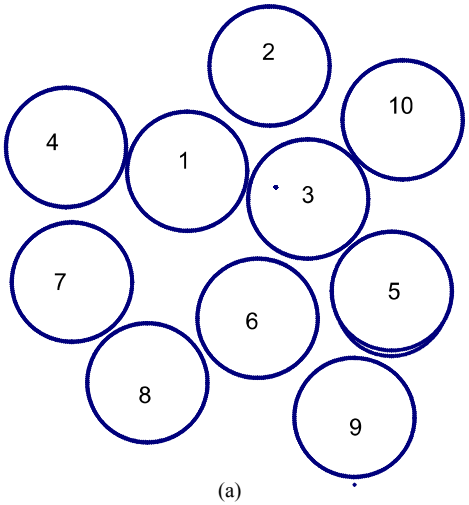

(a)

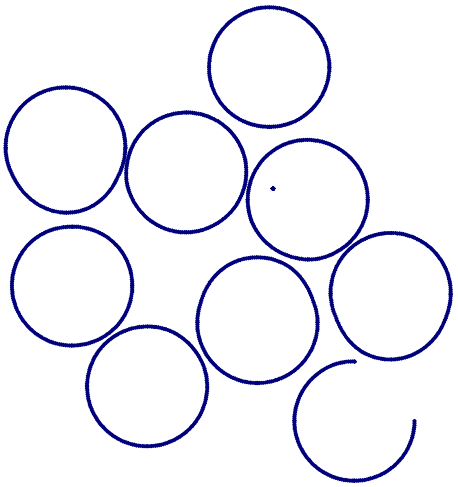

5.2. *Ultimate failure load*

It is also remarkable that, in this particular case, the critical load σ_{cy}^{∞} not only produces the first fibre debond but it also produces the six subsequent fibre debonds, since lower loads are needed when these debonds are produced.

However, for different values of the biaxiality ratio μ and for different rotations of the fibre bundle, sometimes the same behaviour is obtained (σ_{cy}^{∞} produces more than one debond) while in other cases a larger load is necessary to produce the following debonds. Nevertheless, this load is at most 12 % larger than σ_{cy}^{∞}.

Thus, it can be said that σ_{cy}^{∞} value give us an approximation of the failure load in the problem under study (load necessary to produce a macro-crack).

5.3. *Failure curves*

From all the cases solved numerically by BEM for different values of the biaxiality ratio μ and for different rotations of the fibre bundle, it is possible to obtain points in the failure curves for the problem of ten circular inclusions under biaxial transversal loads. These failure curves are shown in Figure 4, the present BEM results are represented by the (color) lines with marks, while the continuous (black) line is a previous result obtained numerically with the single fibre (SF) model, see [11]. Note that the failure curve for the single fibre model can be also analytically obtained by the use of the algorithm developed in [11] which combines an analytical solution in-

troduced in [10] and the LEBI failure criterion. Nevertheless, this analytical solution can not be applied for the multifibre case.

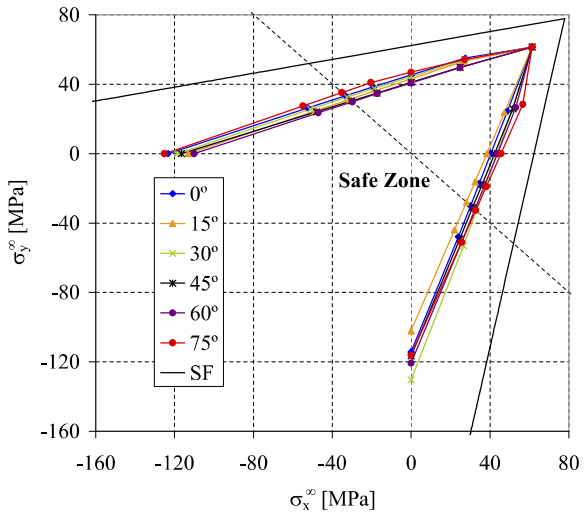

Figure 4: Failure curves for the single fibre (SF) and multifibre models with the fibre bundle rotated different angles with respect to the x-axis.

In Figure 4 each mark on a failure curve is related to a different value of μ. A rotation of the fibre bundle give us a new failure curve. Notice that there are small variations between the failure curves obtained for different rotation angles. After observing the different deformed shapes including fibre-matrix debonds produced in the solved cases, it appears that the values of the critical loads σ_{cx}^{∞} and σ_{cy}^{∞}, for which a new debond initiates typically at one fibre of a pair of close neighbour fibres, are related to the proximity between these neighbour fibres but also taking into account the angle between the load direction and the line segment joining the centers of these fibres. Hereinafter, such a a pair of neighbour fibres will be referred to as critical pair. Thus, if we apply a load in a different direction (obtained by rotating the fibre bundle) the position of the critical pairs of fibres may change nonetheless leading to small changes in the failure curves.

As can be clearly seen in Figure 4, the failure loads for the fibre bundle are lower than the failure loads obtained in the single fibre model. Nevertheless, the results obtained in the present multifibre model confirm some conclusions derived from the results obtained for single fibre model. In particular, when the compression load in the x-direction is larger and keeping constant the tension load in the y-direction (μ tends to values smaller than 0.5), the load necessary for initiating the debond cracks (σ_{cy}^{∞}) is smaller. In other words, compressions in the x-direction make easier crack onset. On the other hand, as can be seen from these results, when the tension load in the x-direction is larger and keeping constant the tension load in the y-direction (μ tends to values bigger than 0.5), the load necessary for a crack onset (σ_{cy}^{∞}) is also larger.

6. CONCLUSIONS

A Linear Elastic-Brittle Interface Model (LEBIM) is used in the present work to study a fibre-matrix debond problem in composite materials. Specifically, this model has been used to characterize the concurrent onset and growth of the debonds in a fibre bundle embedded in an infinite matrix subjected to far field biaxial transverse loads. The problem of ten circular inclusions under biaxial transverse loading assuming material properties of a common composite material (glass fibre and epoxy matrix) and a LEBIM has been solved by the collocational BEM.

From the numerical results it can be seen that after reaching a critical load, the interface crack growth becomes unstable. A serie of picks and valleys appear each one corresponding to a fibre debond. The sequence of the obtained debonds clearly tends to form a macro-crack if the coalescence of these interface cracks may occur.

Sometimes after reaching the critical loads more than one debond is produced for the same load while in other cases a larger load is necessary to produce the following debonds. Nevertheless, this load was at most 12 % larger than the critical load. Thus, it can be said that the critical load value for the first debond onset give a quite good approximation of the failure load of the problem under study (the load necessary to produce a macro-crack).

The critical loads σ_{cx}^{∞} and σ_{cy}^{∞} seems to be related with the relative proximity among fibres (taking into account the load direction). The failure load values for the fibre bundle are lower than the failure loads produced in the single fibre model.

A study of the influence of the load biaxiality ratio μ has also been carried out. BEM results show that compressions in the x-direction enables crack onset for lower tension loads in the y-direction. The presence of tensions in the x-direction implies that larger loads in the y-direction are required to cause crack onset. From all the cases solved numerically by BEM a failure curve for a group of circular inclusions under biaxial transversal loads has been obtained.

The present numerical results confirm the conclusions of the previous studies of fibre-matrix debond under biaxial transverse loading in [1, 2, 3, 4, 5]. The novelty of the present model based on the LEBI formulation consists in its capability of quantitative predictions about the concurrent fibre-matrix debond onset and mixed-mode growth in a fibre bundle.

ACKNOWLEDGEMENTS

The work was supported by the Junta de Andalucía (Projects of Excellence TEP-1207, TEP 02045 and P08-TEP 04051), the Spanish Ministry of Education and Science through Project TRA2006-08077 and MAT2009 - 140022.

REFERENCES

[1] F. París, E. Correa, and J. Cañas. Micromechanical view of failure of the matrix in fibrous composite materials. *Composites Science and Technology*, 63:1041–1052, 2003.

[2] E. Correa. *Micromechanical study of the "matrix failure" in fiber reinforced composites (in Spanish)*. PhD. Thesis, Universidad de Sevilla, 2008.

[3] E. Correa, F. París, and V. Mantič. Tension dominated inter-fibre failure under bi-directional loads. Micromechanical approach. *COMATCOMP 2009, V International Conference on Science and Technology of Composite Materials and 8° Congreso Nacional de Materiales Compuestos, San Sebastián*, pages 915–918, 2009.

[4] E. Correa, F. París, and V. Mantič. Interfacial fracture mechanics approach to the tension dominated inter-fibre failure under bi-directional loads. *ICCM-17, 17th International Conference on Composite Materials (CD), The British Composites Society, Edinburgh*, page 10, 2009.

[5] V. Mantič and I.G. García. Crack onset and growth at the fibre–matrix interface under a remote biaxial transverse load. Application of a coupled stress and energy criterion. *International Journal of Solids and Structures*, 49:2273–2290, 2012.

[6] F. París and J. Cañas. *Boundary Element Method, Fundamentals and Applications*. Oxford University Press: Oxford, 1997.

[7] V. Mantič, A. Blázquez, E. Correa, and F. París. *Analysis of interface cracks with contact in composites by 2D BEM, In: Fracture and Damage of Composites, M. Guagliano and M. H. Aliabadi (Eds.)*, volume 8, pages 189–248. WIT Press: Southampton, 2006.

[8] F. París, E. Correa, and V. Mantič. Kinking of transverse interface cracks between fiber and matrix. *Journal of Applied Mechanics*, 74:703–716, 2007.

[9] L. Távara. *Damage initiation and propagation in composite materials. Boundary element analysis using weak interface and cohesive zone models*. PhD Thesis. Universidad de Sevilla: Sevilla, 2010.

[10] L. Távara, V. Mantič, E. Graciani, and F. París. BEM analysis of crack onset and propagation along fiber-matrix interface under transverse tension using a linear elastic-brittle interface model. *Engineering Analysis with Boundary Elements*, 35:207–222, 2011.

[11] V. Mantič, L. Távara, A. Blázquez, E. Graciani, and F. París. Crack onset and growth at fibre-matrix interface under biaxial transverse loads using a linear elastic-brittle interface model. *Composites Science and Technology, submitted*.

[12] E. Graciani, V. Mantič, F. París, and A. Blázquez. Weak formulation of axi-symmetric frictionless contact problems with boundary elements: Application to interface cracks. *Computer and Structures*, 83:836–855, 2005.

[13] L. Távara, V. Mantič, E. Graciani, and F. París. A BEM analysis of the fibre size effect on the debond growth along the fibre-matrix interface. *Advances in Boundary Element Techniques XI, EC Ltd, Eastleight*, (474–481), 2010.

[14] S. Lenci. Analysis of a crack at a weak interface. *International Journal of Fracture*, 108:275–290, 2001.

[15] A. Carpinteri, P. Cornetti, and N. Pugno. Edge debonding in FRP strengthened beams: Stress versus energy failure criteria. *Engineering Structures*, 31:2436–2447, 2009.

[16] L. Távara, V. Mantič, E. Graciani, J. Cañas, and F. París. Analysis of a crack in a thin adhesive layer between orthotropic materials. An application to composite interlaminar fracture toughness test. *Computer Modeling in Engineering and Sciences*, 58(3):247–270, 2010.

[17] JW. Hutchinson and Z. Suo. *Mixed mode cracking in layered materials*, volume 29 of *Advances in Applied Mechanics*. Academic Press: New York, 1992.

[18] V. Mantič. Interface crack onset at a circular cylindrical inclusion under a remote transverse tension. Application of a coupled stress and energy criterion. *International Journal of Solids and Structures*, 46:1287–1304, 2009.

[19] H. Zhang, ML. Ericson, J. Varna, and LA. Berglund. Transverse single-fiber test for interfacial debonding in composites: 1. Experimental observations. *Composites Part A: Applied Science and Manufacturing*, 28A:309–315, 1997.

[20] J. Varna, LA. Berglund, and ML. Ericson. Transverse single fiber test for interfacial debonding in composites 2: Modelling. *Composites Part A: Applied Science and Manufacturing*, 28:317–326, 1997.